agent: Os-d_2, was obtained in 50% yield; ¹H NMR, Figure 5.

Preparation of 3Re-d_2. One milliliter of D_2O was added to a 3 mL of acetone-d_6 containing 50 mg (0.049 mmol) of [ReDH₃(dppe)₂]Cl[62] prepared by protonation of ReH₃(dppe)₂ with aqueous DCl solution in benzene. The ¹H NMR spectrum of this mixture after 1 week indicated a composition close to [ReD$_{2.7}$H$_{1.3}$(dppe)₂]Cl. The solution was evaporated to dryness in vacuo. The residue was redissolved in 3 mL of THF and then reacted with 2 mL of 1.6 M *n*-BuLi in hexane. After the reaction mixture was stirred for 10 min, 2 mL of EtOH were added to neutralize the excess BuLi. The solvent was removed under vacuum, and the residue was extracted with benzene. The benzene was removed under vacuum, and the yellow residue was washed with 2 mL of EtOH to give a yellow powder. The powder was collected by filtration, washed with EtOH, and dried in vacuo overnight: yield 34 mg, 68%. Integration of resonances in the ¹H NMR spectrum gave the composition ReD$_{2.2}$H$_{0.8}$-(dppe)₂.

Preparation of trans-[Os(CO)H(dppe)₂]BF₄. 1Os was prepared in situ from 0.085 g (0.086 mmol) of OsH₂(dppe)₂ and HBF₄·Et₂O. The reactant was dissolved in 15 mL of acetone yielding a clear solution. The solution was degassed with CO and allowed to stir under CO for 31.5 h. A ³¹P NMR spectrum indicated that H_2 displacement was complete. After obtaining ¹H NMR and IR spectra the remaining product was crystallized from acetone by slow Et₂O diffusion: IR (CH₂Cl₂) ν(CO) 2002.5 s, ν(OsH) 1916.5 cm⁻¹ w; δ(¹H, acetone-d_6) -7.87 (quint, J_{HP} = 19.2 Hz, 1 H), δ(³¹P, acetone) 30.4 (s). Anal. Calcd for C₅₃H₄₉BF₄OOsP₄: C, 57.77; H, 4.47. Found: C, 57.37; H, 4.52.

Reaction of 2Os with Carbon Monoxide. The complex (0.091 g, 0.098 mmol) in 10 mL of acetone at 20° was reacted with CO (1 atm). The rate of loss of 2Os was monitored by ³¹P NMR and shown to be first order in [2Os] with $t_{1/2}$ = 170 h. *trans*-[OsH(depe)₂(CO)]⁺ [34] was the only product: δ(³¹P, acetone) 27.7 (s).

Note Added in Proof. Brammer et al.[66] have reported an "intermediate" H–H distance of 1.357 (7) Å in the complex ReH₇(Ptol₃)₂. This was a single-crystal neutron diffraction study. Thus structure **2**, Figure 1, is feasible for complex **2Os**. It is not yet known whether this Re complex will have T_1 and J(H,D) coupling behavior similar to that of **2Os-d_2**.

(66) Brammer, L.; Howard, J. A. K.; Johnson, O.; Koetzle, T. F.; Spencer, J. L.; Stringer, A. M. *J. Chem. Soc., Chem. Commun.*, in press.

Multifield Saturation Magnetization and Multifrequency EPR Measurements of Deoxyhemerythrin Azide. A Unified Picture

Michael P. Hendrich,† **Linda L. Pearce,**‡ **Lawrence Que, Jr.,**‡ **N. Dennis Chasteen,**§ **and Edmund P. Day*,†**

Contribution from the Gray Freshwater Biological Institute, University of Minnesota, Navarre, Minnesota 55392, the Department of Chemistry, University of Minnesota, Minneapolis, Minnesota 55455, and the Chemistry Department, University of New Hampshire, Durham, New Hampshire 03824. Received September 27, 1990

Abstract: The magnetic properties of deoxyhemerythrin azide have been measured by combining multifield saturation magnetization data and multifrequency EPR spectra. The exchange coupling [J = -3.4 (1) cm⁻¹; $JS_1 \cdot S_2$], average zero-field splitting parameters [$|D_1| = |D_2|$ = 12 (1) cm⁻¹ and $E_1/D_1 = E_2/D_2$ = 0.3], and average g values [$g_1 = g_2$ = 2.23 (5)] have been determined assuming identical iron sites with parallel zero-field splitting axes for the ferromagnetically coupled high-spin diferrous center. The observed ratio of the exchange coupling to the zero-field splitting (J/D_i = 0.28) lies in the weak exchange coupling regime of a perturbation treatment of the full 25 × 25 spin Hamiltonian of the coupled diiron center. Perturbation expressions required for the description of the integer-spin EPR signals of two S = 2 metals in either the strong ($J/D_i > 1$) or weak ($J/D_i < 1/3$) exchange coupling regimes are presented. For deoxyhemerythrin azide the EPR signal arises from the lowest pair of energy levels of the coupled system and can be interpreted in either coupling regime. The saturation magnetization family of curves, on the other hand, are a thermal average of all levels populated from 2 to 200 K and can resolve this ambiguity in the interpretation of the EPR data. An excellent fit to the entire family of multifield saturation magnetization curves has determined both the exchange coupling and zero-field splitting of deoxyhemerythrin azide, which lies in the weak coupling regime. In addition, quantitative agreement between saturation magnetization, integer-spin EPR, and optical data has been obtained.

Hemerythrin is a well-characterized oxygen-storage protein isolated from several marine organisms.[1,2] For deoxyhemerythrin the active site consists of two high-spin iron atoms that are bridged by a hydroxo group[3,4] and two carboxolato groups, one each from an aspartate and a glutamate residue.[5] Five of the remaining coordination sites of the diiron center are histidine residues, leaving a single coordination site available for exogenous ligands. In deoxyhemerythrin the two high-spin ferrous ions are antiferro-

magnetically coupled with J estimated to be between 20 and 70 cm⁻¹ ($JS_1 \cdot S_2$).[1,2,4,6,7] Reem and Solomon showed, in studies combining magnetic circular dichroism (MCD) and EPR, that upon addition of azide to deoxyhemerythrin the exchange coupling

* Address correspondence to this author at the Department of Physics, Emory University, Atlanta, GA 30322.
† Gray Freshwater Biological Institute, University of Minnesota.
‡ Department of Chemistry, University of Minnesota.
§ Chemistry Department, University of New Hampshire.

(1) Klotz, I. M.; Kurtz, D. M., Jr. *Acc. Chem. Res.* **1984**, *17*, 16–22.
(2) Wilkins, P. C.; Wilkins, R. G. *Coord. Chem. Rev.* **1987**, *79*, 195–214.
(3) Reem, R. C.; Solomon, E. I. *J. Am. Chem. Soc.* **1984**, *106*, 8323–8325.
(4) Zhang, K.; Stern, E. A.; Ellis, T.; Sanders-Loehr, J.; Shiemke, A. K. *Biochemistry* **1988**, *27*, 7470–7479.
(5) Stenkamp, R. E.; Sieker, L. C.; Jensen, L. H.; McCullum, J. D.; Sanders-Loehr, J. *Proc. Natl. Acad. Sci. U.S.A.* **1985**, *82*, 713–716.
(6) Maroney, M. J.; Kurtz, D. M.; Nocek, J. M.; Pearce, L. L.; Que, L. *J. Am. Chem. Soc.* **1986**, *108*, 6871–6879.
(7) Reem, R. C.; Solomon, E. I. *J. Am. Chem. Soc.* **1987**, *109*, 1216–1226.

becomes ferromagnetic ($|J| > 2$ cm^{-1}).[7] They suggested that the hydroxo bridge had become protonated to form an aqua bridge.[3]

Here we report multifield saturation magnetization data and both X-band and Q-band integer-spin EPR signals of deoxyhemerythrin azide. We have developed new methods for analyzing integer-spin EPR signals that allow quantitative comparison of these data. A single description of the coupled diferrous site will be presented that is consistent with both the magnetization and EPR data but differs from the previous description based on MCD and EPR data.[7]

There are now a variety of metalloproteins and synthetic model complexes that show integer-spin EPR signals. The core metal units of these complexed are iron porphyrin,[8,9] Fe–O–Fe,[3,7,8,10–13] Fe–O–Cu,[8,14–16] [Fe$_3$S$_4$],[17–19] iron thiolate,[20] and Mn–O–Mn.[21] Very few of these signals have been quantitatively analyzed. The EPR signal from deoxyhemerythrin azide is of particular interest for a number of reasons. The protein has been well studied and the concentration can be determined optically. The integer-spin EPR signal of deoxyhemerythrin azide is identical with that of the synthetic model complex [Fe$_2$BPMP(O$_2$CR)$_2$]BPh$_4$;[13] such close similarities are rare. An integer-spin EPR signal from methane monooxygenase[11] has recently been characterized by the present techniques. This study of deoxyhemerythrin azide, which combines multifield saturation magnetization data with integer-spin EPR spectra, provides a check on the validity of the methane monooxygenase study, which was based on integer-spin EPR spectroscopy alone. We show here that integer-spin EPR signals of this class of proteins can be reliably and accurately quantitated.

Experimental Methods

Oxyhemerythrin was isolated and crystallized[22] from marine worms of the species *Phascolopsis gouldii* obtained live from the Marine Biological Laboratory, Woods Hole, MA. Deoxyhemerythrin was prepared by anaerobic dialysis for several days at 4 °C against 1.0 mM ethylenediaminetetraacetate (EDTA), 20 mM 2-(N-morpholino)ethanesulfonic acid (MES), pH 6.0, 1.0 mM Na$_2$S$_2$O$_4$, and 0.1 M Na$_2$SO$_4$. Deoxyhemerythrin azide was prepared by the anaerobic addition of a 200-fold excess of NaN$_3$ to deoxyhemerythrin. The protein concentration was measured spectrophotometrically after allowing deoxyhemerythrin azide to oxidize in air for 24 h at 4 °C to methemerythrin azide (ϵ_{446} = 3700 M^{-1} cm^{-1} [23]).

Three samples ($\approx$1 mL of protein solution) were prepared by anaerobic exchange into 100 mL of a deuterated (99%) buffer at pD = 6.5 (pH reading + 0.4). Sample 1 (2.4 mM deoxyhemerythrin azide) was prepared as above with the addition of 10% glycerol. Sample 2 (3.5 mM) and sample 3 (1.6 mM) were prepared without glycerol.

Magnetization samples were prepared from samples 1 and 2. No significant difference in the saturation magnetization of these samples was observed, indicating that glycerol did not significantly affect the magnetic properties of deoxyhemerythrin azide. Protein samples of 180 µL were loaded anaerobically with a calibrated pipet into Suprasil quartz

buckets that had been etched overnight in 10% hydrofluoric acid to remove ferromagnetic impurities. Controls were made in each case by anaerobically adding 180 µL of protein dialyzate to a quartz bucket matched in weight to that of the sample. EPR samples were prepared from samples 2 and 3. Samples and controls in the uncapped quartz holders were then frozen in liquid nitrogen and kept frozen until completion of the magnetization or EPR study.

Multifield saturation magnetization data were collected as described previously[24] with a Quantum Design superconducting susceptometer from 2 to 200 K at fixed fields ranging from 0.2 to 5.5 T. The instrument was modified by the manufacturer to introduce a bleed flow of low-pressure helium gas past the unsealed sample to minimize effects of sample outgassing.

Theoretical powder average magnetization curves were calculated from the spin Hamiltonian of eq 1 as described previously.[24] The saturation magnetization difference data (sample minus control) were fit by the simplex method[25] to find the spin Hamiltonian parameters yielding the minimum in the standard quality of fit parameter, χ^2. Uncertainties in the spin Hamiltonian parameters were found by averaging the results of fitting data collected from the two independently prepared samples. The amount of paramagnetism found from the fitting process was used to scale the vertical axes of Figure 3. The software to carry out this data analysis was developed by Thomas A. Kent.

X-band EPR measurements were performed with a Varian E9 spectrometer using an Oxford liquid helium cryostat. A Varian Model E-236 bimodal cavity was used to generate the microwave magnetic fields parallel and perpendicular to the static field. For the temperature-dependent study, a calibrated carbon glass resistor (CGR-1-1000, Lakeshore Cryotronics) was immersed in the sample. The EPR tube was positioned vertically to minimize impurity signals from the resistor. The leads of the resistor were replaced with a phosphor bronze wire to minimize heat input. To test whether temperature gradients were affecting the results, the measurements were made with sample lengths of both 5 and 20 mm. No significant differences were observed between the data sets. Q-band measurements were performed on a Varian E9 spectrometer using a cylindrical TE$_{110}$ cavity immersed in a helium gas flow. The Q-band dewar with a fiberglass tail section (Cryo Industries of America) gave good temperature stability and allowed 1-mT, 100-KHz, modulation at the sample. An NMR gaussmeter was used to calibrate the magnetic field strength for both the X- and Q-band measurements. In addition, the X-band microwave frequency was measured with a counter.

For quantitation, EPR signals were compared against the signal from a single crystal of zinc fluorosilicate with a 1.5% iron doping. The ratio of iron to zinc was determined by plasma emission spectroscopy and the total number of metal atoms from the weight of the crystal.

Analysis. The energy levels of the system formed by two exchange-coupled, spin $S = 2$ sites can be described by the spin Hamiltonian

$$\hat{H} = J\mathbf{S}_1\cdot\mathbf{S}_2 + \sum_i[D_i(S_{zi}^2 - 2) + E_i(S_{xi}^2 - S_{yi}^2) + \beta S_i\cdot g_i\cdot H] \quad i = 1, 2$$

(1)

where J is the isotropic exchange coupling constant, D_i and E_i are the axial and rhombic zero-field splitting parameters, and g_i are the g tensors of the uncoupled sites ($i = 1, 2$). The standard assumption is made that each D_i zero-field splitting tensor has the same axes as its g_i tensor. Plots of the system's energy levels versus D_i/J have been published.[7] A glance at these plots will quickly convey the complexity of the problem. However, spectroscopic techniques are usually sensitive to a few low-lying spin states and the problem can be simplified with a perturbation treatment that focuses on these low energy levels.

The resonance condition for integer-spin EPR signals is

$$(h\nu)^2 = \Delta^2 + (\tilde{g}\beta H)^2$$

(2)

where the pair of levels absorbing microwave energy at frequency ν are split in zero field by an energy Δ. The spectroscopic splitting factor is $\tilde{g} = g_{\text{eff}} \cos \Psi$, where Ψ is an angle between the static field H and an appropriate molecular axis and g_{eff} is the effective g value along this axis. The EPR spectrum is determined by three quantities: Δ, g_{eff}, and the transition probability (w). In addition, a match to observed EPR line shapes can only be accomplished with distributions in the zero-field parameters, D_i and E_i.[8] We will present expressions for Δ, g_{eff}, and w derived from eq 1 using perturbation theory. The expressions are applicable within two broad exchange-coupled regimes, namely, strong ($|J/D_i| > 1$) and weak ($|J/D_i| < 0.3$).[26] The validity of the calculations has been tested for agreement with diagonalization of the Hamiltonian of eq 1.

(8) Hendrich, M. P.; Debrunner, P. G. *Biophys. J.* **1989**, *56*, 489–506.

(9) Hendrich, M. P.; Debrunner, P. G. *J. Magn. Reson.* **1988**, *78*, 133–141.

(10) Lynch, J. B.; Juarez-Garcia, C.; Münck, E.; Que, L., Jr. *J. Biol. Chem.* **1989**, *264*, 8091–8096.

(11) Hendrich, M. P.; Münck, E.; Fox, B. G.; Lipscomb, J. D. *J. Am. Chem. Soc.* **1990**, *112*, 5861–5865.

(12) Tolman, W. B.; Bino, A.; Lippard, S. J. *J. Am. Chem. Soc.* **1989**, *111*, 8522–8523.

(13) Borovik, A. S.; Hendrich, M. P.; Holman, T. R.; Münck, E.; Papaefthymiou, V.; Que, L., Jr. *J. Am. Chem. Soc.* **1990**, *112*, 6031–6038.

(14) Hagen, W. R. *Biochim. Biophys. Acta* **1982**, *708*, 82–98.

(15) Dunham, W. R.; Sands, R. H.; Shaw, R. W.; Beinert, H. *Biochim. Biophys. Acta* **1983**, *748*, 73–85.

(16) Juarez-Garcia, C.; Hendrich, M. P.; Holman, T. R.; Que, L., Jr.; Münck, E. *J. Am. Chem. Soc.*, in press.

(17) Papaefthymiou, V.; Girerd, J. J.; Moura, I.; Moura, J. J. G.; Münck, E. *J. Am. Chem. Soc.* **1987**, *109*, 4703–4710.

(18) Hagen, W. R.; Dunham, W. R.; Johnson, M. K.; Fee, J. A. *Biochim. Biophys. Acta* **1985**, *828*, 369–374.

(19) Conover, R. C.; Koual, A. T.; Fu, W.; Park, J.; Aono, S.; Adams, M. O. W.; Johnson, M. K. *J. Biol. Chem.* **1990**, *265*, 8533–8541.

(20) Werth, M. T.; Johnson, M. K. *Biochemistry* **1989**, *28*, 3982–3988.

(21) Dexheimer, S. C.; Gohdes, J. W.; Chan, M. K.; Hagen, K. S.; Armstrong, W. H.; Klein, M. P. *J. Am. Chem. Soc.* **1989**, *111*, 8923–8925.

(22) Klotz, I. M.; Klotz, T. A.; Fiess, J. A. *Arch. Biochem. Biophys.* **1957**, *68*, 284–299.

(23) Garbett, K.; Darnell, D. W.; Klotz, I. M.; Williams, R. J. P. *Arch. Biochem. Biophys.* **1969**, *135*, 419–434.
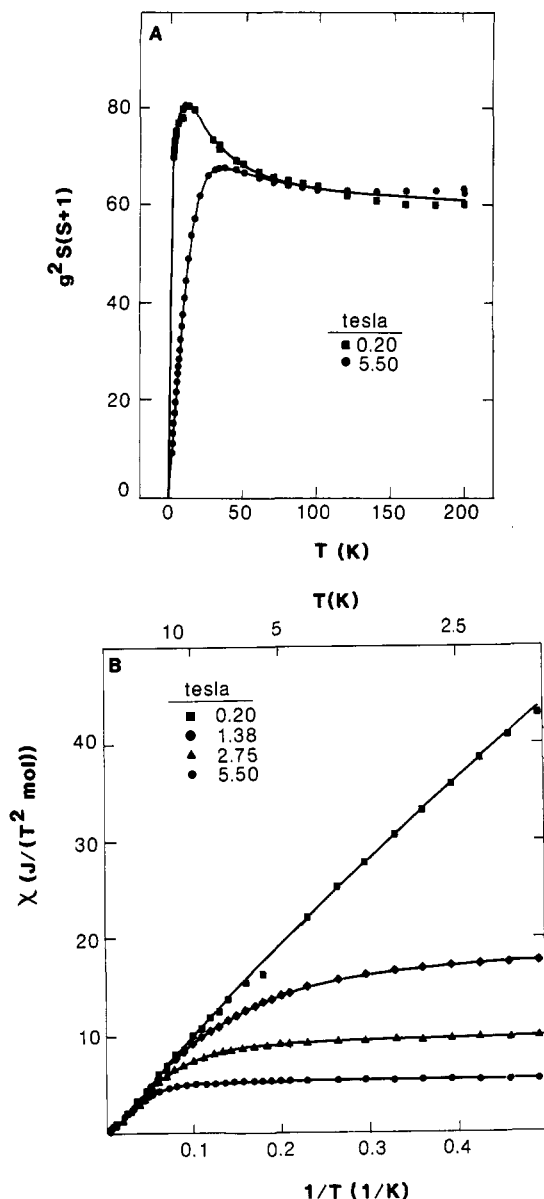
(24) Day, E. P.; Kent, T. A.; Lindahl, P. A.; Münck, E.; Orme-Johnson, W. H.; Roder, H.; Roy, A. *Biophys. J.* **1987**, *52*, 837–853.

(25) Nelder, J.; Mead, R. *Comput. J.* **1965**, 308–313.

(26) This inequality was reversed by a typographical error in ref 11.

Figure 1. Energy levels of an $S = 4$ manifold (strong coupling regime) for $H = 0$ and negative D. The levels have labels appropriate for zero-field states at small E/D values; $|M_s^{\pm}\rangle = (|4,+M_s\rangle \pm |4,-M_s\rangle)/2^{1/2}$. EPR signals near $g = 16$ (assuming $g = 2$ in eq 3) may be observed from the two pairs of levels noted.

Strong Exchange Coupling. For strong exchange coupling, the total spin $S = 0, 1, 2, 3, 4$ multiplets separate, with the lowest being $S = 4$ for ferromagnetic coupling. The energy splittings of the ground $S = 4$ multiplet are shown in Figure 1 and can be described by the spin Hamiltonian

$$\hat{H} = D(S_z^2 - 20/3) + E(S_x^2 - S_y^2) + \beta \mathbf{S} \cdot \mathbf{g} \cdot \mathbf{H} \qquad (3)$$

The coupled **D** and **g** tensors are related to the individual site tensors by the relations $\mathbf{D} = (3/14)(\mathbf{D}_1 + \mathbf{D}_2)$ and $\mathbf{g} = (1/2)(\mathbf{g}_1 + \mathbf{g}_2)$.[27]

For negative D, the lowest pair of states are approximately $|4^{\pm}\rangle = (|S=4,M_s=+4\rangle \pm |S=4,M_s=-4\rangle)/2^{1/2}$. The quantities Δ, g_{eff}, and w are given to a close approximation by the expressions

$$\Delta = (35/16)|D|\alpha^4 \qquad (4a)$$

$$g_{eff} = 8g_{zz}(1 - 7\alpha^2/36) \qquad (4b)$$

$$w = (g_{eff}\beta H_{1z}\Delta/h^2\nu)^2 f(\nu) \qquad (4c)$$

where $\alpha = E/D$ ($0 < \alpha < 1/3$), $f(\nu)$ is the spin-packet line-shape function, and the z axis is the appropriate axis of the zero-field tensor for eq 2. The relations for positive D are obtained from eq 4 by substituting the quantities $(1 - \alpha)/(1 + 3\alpha)$ for α, $(D/2)(1 + 3\alpha)$ for D, and y for z. The lowest pair of states is then $|0\rangle$ and $|1^-\rangle$.

The transition probability w depends on the finite matrix element $\langle 4^+|S_z|4^-\rangle$ ($D < 0$, $E/D \neq 0$), even in the absence of the static magnetic field. Previous authors[7] have required a static field to mix the states and give a nonzero transition probability, with the selection rule $\delta m_s = \pm 1$. This previous treatment is inappropriate for integer-spin (non-Kramers) states, since the dominant interaction splitting the EPR active doublet at low field is the spin–orbit coupling and not the magnetic field. The appropriate selection rules are $\delta m_s = 0, \pm 1$.

The transition probability of eq 4 assumes $f(\nu)$ is normalized, i.e., $\int f(\nu) \, d\nu = 1$. If spectral simulations instead assume a normalized spin packet as a function of magnetic field $b(H)$, then the substitution $f(\nu) = b(H)(dH/d\nu)$ is made. The derivative can be calculated from eq 2 and we have found a δ function spin packet, $b(H) = \delta(H)$, to be sufficient in previous work.[8,9,11,16]

The energy splitting to the next excited doublet, $7D$ for $E/D = 0$, can be determined from a study of the temperature dependence of the intensity of the ground doublet. If favorable relaxation conditions persist at higher temperatures, the excited doublet may give an additional resonance near $g_{eff} = 12$. The remaining parameters of eq 4 are determined by spectral simulations. The simulations also provide a normalization factor that allows quantitation of the spectrum. Rotations of the individual $\mathbf{D}_i$ tensors, which may also have different magnitudes, will not affect the parameter values or quantitation results. Information about

(27) Scaringe, R. P.; Hodgson, D. K.; Hatfield, W. E. *Mol. Phys.* **1978**, *35*, 701–713.

Figure 2. Effect of a weak exchange interaction on the $|2^{\pm}\rangle$ states of two $S = 2$ sites (weak coupling regime). The diagram assumes the zero-field splitting tensors have parallel axes with negative D_i and $E_i/D_i \approx 0$. For clarity, the effect of coupling on the higher energy $|0\rangle$ and $|1^{\pm}\rangle$ states is not shown. For ferromagnetic coupling, the EPR-active doublet of the quartet shown is low in energy; for antiferromagnetic coupling the EPR-active doublet is high energy.

the individual $\mathbf{D}_i$ tensors and their spatial relations is lost in the strong coupling regime.

Weak Exchange Coupling. We now consider the other exchange regime, where the zero-field splitting parameters are overall larger than the exchange coupling. For this case, it is convenient to work in the uncoupled basis $|S_1 S_2 m_1 m_2\rangle$ and treat the exchange coupling as a perturbation on these states. The effect of the exchange coupling on the lowest four states is shown in Figure 2 for negative D_i and $E_i/D_i \approx 0$. The lowest pair of states, $|2^{\pm}\rangle = (|+2\rangle \pm |-2\rangle)/2^{1/2}$, of both $S = 2$ quintets couple to form a quartet. The quartet is split by the exchange interaction into two doublets separated in energy by $8J$ for $E_i/D_i = 0$, as shown in Figure 2. Interestingly, the doublets have different magnetic properties; e.g., only one is EPR active. For ferromagnetic coupling the EPR-active doublet is low. For equal $\mathbf{D}_i$ tensors having parallel axes, the parameters that determine the spectrum of the EPR-active doublet are to a good approximation given by

$$\Delta = [\Delta_1^2 + (4a_1^2 J)^2]^{1/2} - 4a_1^2 J \approx \Delta_1^2/8J \qquad (5a)$$

$$g_{eff} = 4a_1 g_{zz1}(A^+ + A^-) \qquad (5b)$$

$$w = (g_{eff}\beta H_{1z}\Delta/h^2\nu)^2 f(\nu) \qquad (5c)$$

where $a_1^2 = (1/2)(1 + [1 + 3\alpha_1^2]^{-1/2})$, $A^{\pm} = (1 \pm \Delta_1[\Delta_1^2 + (4a_1^2 J)^2]^{-1/2})^{1/2}$, and the splitting of the uncoupled $|2^{\pm}\rangle$ doublet is $\Delta_1 = 2D_1([1 + 3\alpha_1^2]^{1/2} - 1)$. The mixing functions a_1 and $A^{\pm}$ are due to the rhombic and exchange interactions, respectively. Equation 5 assumes D_i is negative and the appropriate axis for eq 2 is along z.

In the weak coupling regime the exchange coupling is determined from a fit to the temperature dependence of the EPR data. If favorable relaxation conditions persist to higher temperatures, the analysis will give an indication of the D_i value as well.

The particular values for D_i, α_i, and g_{zzi} obtained from spectral simulation and fits to the temperature-dependent data will change if the $\mathbf{D}_i$ tensors are allowed to be unequal and tilted. (For $D_1 \neq D_2$, the splitting of the EPR-active doublet is $\Delta \approx \Delta_1 \Delta_2/8J$.) However, the new values must produce the same g_{eff} and Δ for matching spectral simulations. Thus the transition probability, and consequently the quantitative results, should not be affected.

Results

The integer-spin EPR signal of the azide complex of deoxyhemerythrin is sensitive only to the lowest energy levels of the coupled iron site and can be interpreted in either the strong coupling or the weak coupling regimes presented above. On the other hand, a family of multifield saturation magnetization curves presents a thermal average of all levels populated between 2 and 200 K at fields from 0.2 to 5.5 T. These saturation magnetization data resolve the ambiguity in the interpretation of the integer-spin EPR signals and will be presented first.

Magnetization data of deoxyhemerythrin azide (sample 2) collected at four fixed fields (5.5, 2.75, 1.375, and 0.2 T) over the temperature range from 2 to 200 K are shown in Figure 3. In Figure 3A the data are presented as μ_{eff}^2 versus temperature

Figure 3. Magnetization of deoxyhemerythrin azide (sample 2) at four fixed fields over the temperature range 2–200 K. (A) The extreme fields plotted as μ_{eff}^2 versus temperature. (B) All four fields plotted as susceptibility ($\chi = M/H$) versus inverse temperature. The solid lines were calculated by diagonalizing the full 25 × 25 spin Hamiltonian of eq 1, assuming identical ferrous sites having parallel axes for the zero-field splitting tensors with $D_i = 12$ cm^{-1}, $E_i/D_i = 0.31$, and $g_i = 2.25$ and with $J = -3.4$ cm^{-1}.

at the extreme fields. In Figure 3B the data are presented as susceptibility ($\chi = M/H$) (in SI units) versus inverse temperature at all four fields. In combination these two plots clearly exhibit the quality of the data and the fit at both ends of the temperature range. The rise from horizontal with decreasing temperature in Figure 3A graphically indicates ferromagnetic coupling. It is this feature in the data that determines the sign and magnitude of the exchange coupling and that resolves the ambiguity in the interpretation of the integer-spin EPR signal.

The solid lines in Figure 3 were calculated by diagonalization of the full 25 × 25 spin Hamiltonian of eq 1 with $J = -3.4$ (1) cm^{-1}, $|D_1| = |D_2| = 12$ (1) cm^{-1},[28] $E_1/D_1 = E_2/D_2 = 0.31$ (1), and $g_1 = g_2 = 2.23$ (5). The uncertainties in parentheses were arrived at by averaging the parameters from the best fits to two independently prepared samples. The EPR spectra of sample 2 (whose

---

(28) The absolute value of D_i is specified because the sign of D_i is ambiguous for $E_i/D_i \approx {}^1/_3$.

H(mT)
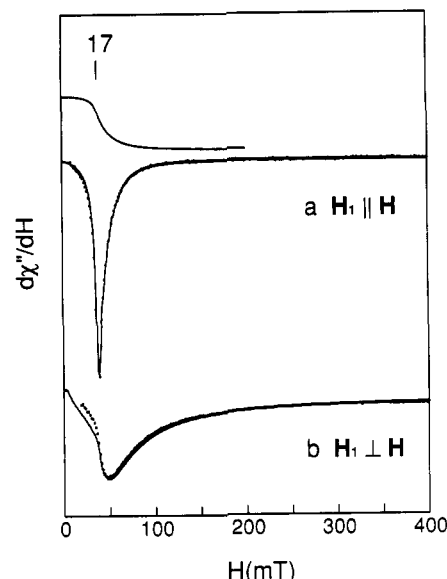
Figure 4. X-band (9.16 GHz; 2 μW) EPR spectra (—) and simulations (···) of deoxyhemerythrin azide (sample 2) at 4 K using a microwave field H_1 (a) parallel and (b) perpendicular to the static field **H**. The truncated spectrum above (a) is a digital integral of the experimental spectrum of (a). The simulations are based on the weak coupling perturbation expression (eq 5), assuming identical ferrous sites with parallel axes for the zero-field splitting tensors and with $D_i = -10$ cm^{-1}, $E_i^0 = 3$ cm^{-1}, $\sigma_E = 0.8$ cm^{-1}, and $g_{zzi} = 2.20$ for the ground doublet with $J = -3$ cm^{-1}. There are no adjustable parameters between the simulations of (a) and (b); that is, eq 13 of ref 8 is obeyed.

H(mT)
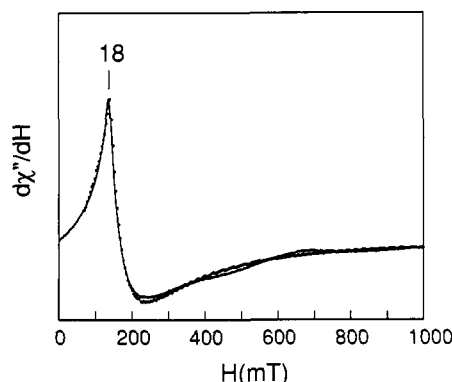
Figure 5. Q-band (34.3 GHz; H_1 perpendicular to H) EPR spectrum (—) and simulation (···) of deoxyhemerythrin azide at 5 K. The simulation parameters are identical with those of Figure 4.

magnetization data are shown in Figure 3) can be interpreted from either of two different parameter sets, thus efforts were made to find a second fit to the saturation magnetization data. No other fit was found under the assumption of identical sites with parallel axes for the zero-field splitting tensors.[29]

The measured value for J/D is 0.28 from the saturation magnetization data. This places the azide complex of deoxyhemerythrin in the weak coupling regime (eq 5 and Figure 2). EPR spectra and simulations in the weak coupling regime at X- (0.3 cm^{-1}) and Q- (1.2 cm^{-1}) band are shown in Figures 4 and 5. The spectra were recorded at 4 K with the magnetic microwave field (H_1) either parallel or perpendicular to the static field (**H**).

---

(29) We now have a computer program, written by Thomas A. Kent, which searches thoroughly within the specified bounds of each spin Hamiltonian parameter of eq 1 for the best (least χ^2) fit to the multifield saturation magnetization data. In the present case there were just four free parameters ($D_1 = D_2$; $E_1/D_1 = E_2/D_2$; $g_1 = g_2$; and J) and the search included ten randomly generated starting points in addition to our initial guess. In addition, fits were attempted with the parameters locked to those found in the strong coupling regime, which simulated the integer-spin EPR spectra. The best fit consistent with the strong coupling regime had a χ^2 more than 18 times larger (i.e., a very poor fit) than that of the fit shown in Figure 3.

Measurements of Deoxyhemerythrin Azide

J. Am. Chem. Soc., Vol. 113, No. 8, 1991 3043

Table I. Protein Concentration of Deoxyhemerythrin Azide Samples

sample	concentration, mM		
	optical	magnetization	EPR
1	2.4	2.1[a]	
2	3.5	2.8[a]	4.0
3	1.6		1.7

[a] Magnetization measures the product g^2(concentration)(volume). g^2 is found from the shape of the family of magnetization curves in the saturation region. Because uncertainty in g^2 correlates inversely with the concentration measurement, a g value of 1.99 for sample 2 instead of the value 2.25 found from the fit would yield the same concentration as that measured optically.

The position of the valley in the parallel mode (Figure 4a) is at $g = 17$ ($g = h\nu/\beta H$). The derivative spectra, both plotted on the same scale, show a significant signal enhancement in the parallel mode, $I_\parallel/I_\perp = 3$ (measured zero to valley), as is typical for integer-spin EPR spectra. An integral of the parallel mode spectrum (truncated spectrum above Figure 4a) shows finite signal intensity at zero field. This result is indicative of a broad distribution in the zero-field splitting Δ. Some molecules of the sample have $\Delta = h\nu$ and thus, in accordance with eq 2, will resonate at precisely $H = 0$. Another fraction of the molecules has a larger zero-field splitting $\Delta > h\nu \approx 0.3$ cm^{-1}; the resonance condition cannot be satisfied for these molecules at any field H with an X-band spectrometer. Thus, these molecules do not contribute to the signal. The fraction of unobserved molecules is significantly reduced for spectra of Figure 5 taken at Q-band ($h\nu \approx 1.2$ cm^{-1}). The perpendicular Q-band spectrum spans more than 1 T and is broad like the corresponding X-band spectrum, Figure 4. The position of the peak is at $g = 18$. (The positions of the peak in Figure 5 or the valley in Figure 4b are not necessarily equal to g_{eff} of eq 1 since nonzero values for Δ will shift each feature to lower field and give $g > g_{eff}$.)

Figure 6 shows the temperature dependence of the signal of Figure 4b plotted as signal amplitude times temperature versus temperature. The data show that the EPR-active doublet is the ground state, in agreement with previous findings.[7] A simple three-doublet analysis of the depopulation of the ground doublet indicates the next excited doublet is at 20 cm^{-1}.

The EPR data can be described in either the strong or weak coupling regimes. However, the magnetization data indicate that deoxyhemerythrin azide is weakly coupled. Therefore, we will analyze the EPR results in the weak coupling limit under the assumption of equal D_i tensors with parallel axes. The best fit to the temperature data for $E_i/D_i = 0.3$ is shown in Figure 6 and gives $J = -3$ cm^{-1} and $|D_i| = 10$ cm^{-1}.[30] The curve is generated from diagonalization of eq 1, but a close value for J can be obtained from the energy splitting to the next excited doublet, $|J| \approx 20$ cm$^{-1}/8 = 2.5$ cm^{-1}. From simulations based on eq 5, the parameters required for simultaneous fits to both the X- and Q-band data of Figures 4 and 5 are negative D_i, $E_i/D_i = 0.3$, $\sigma_{E/D} = 0.08$, and $g_{zzi} = 2.20$. The broad spectral line shapes are adequately modeled with a Gaussian distribution of E_i values, centered at E_i^0 with width σ_E (one standard deviation). A distribution in the D_i value has little effect since $(d\Delta/dE_i)/(d\Delta/dD_i) = 6$ at $E_i/D_i = \frac{1}{3}$. The fraction of molecules with $\Delta < h\nu \approx 0.3$ cm^{-1}, and thus observed in the X-band spectra, is 50%; for Q-band the fraction is 95%. The intensity and line shape of the perpendicular mode spectrum of Figure 4b are correctly determined from a fit to the parallel mode spectrum of Figure 4a without the use of any adjustable parameters.

The EPR signals of Figures 4 and 5, including the intensity, are now completely specified using parameters consistent with the saturation magnetization data. To check the analysis, the X-band spectral intensity of deoxyhemerythrin azide was compared to a standard, iron fluorosilicate, having a known number of spins. The results are shown in Table I in comparison with optical and magnetization measurements for three samples. These results were

(30) The best value for D_i from analysis of the EPR data is below that measured by the magnetization data but within the experimental uncertainties.

obtained from EPR spectra recorded with nonsaturating microwave power. The shape of the integer-spin EPR signal of deoxyhemerythrin azide is altered with modest amounts of microwave power,[8] contrary to a previous report.[7] Saturated signals will give both inaccurate quantitation and inaccurate temperature data.

Discussion

The ferromagnetic exchange coupling [$J = -3.4$ (1) cm^{-1}; $JS_1 \cdot S_2$], zero-field interactions [$|D_1| = |D_2| = 12$ (1) cm^{-1} [28] and $E_1/D_1 = E_2/D_2 = 0.3$], and average g values [$g_1 = g_2 = 2.23$ (5)] of deoxyhemerythrin azide have been determined assuming identical ferrous sites with parallel axes for the zero-field splitting tensors. This spin Hamiltonian parameter set describes both the multifield saturation magnetization family of curves and the integer-spin EPR signals at both X- and Q-band. In addition the EPR data give a value for $g_{zz1} = g_{zz2} = 2.20$ (5) and indicate a broad distribution in the zero-field splitting parameters. The saturation magnetization data have been used to measure the exchange coupling, which is weak relative to the zero-field interaction ($J/D_i \approx 0.28$). To our knowledge, this is the first diferrous complex for which these quantities have been determined. The results show quantitative agreement between multifield saturation magnetization, multifrequency integer-spin EPR, and optical data. The quantitative agreement and simultaneous fit to the saturation magnetization family of curves has provided an important check on the method of analysis of the EPR data. The agreement strengthens our confidence in the interpretation of the integer-spin EPR signals of the diferrous site of methane monooxygenase,[11] where this same analysis was applied but data from magnetization and Mössbauer measurements are not yet available.

The low-temperature MCD and the X-band perpendicular mode integer-spin EPR signal of deoxyhemerythrin azide have previously been analyzed by Reem and Solomon.[7] We are in agreement with their finding of ferromagnetic coupling in this complex. However, we disagree that there is an excited doublet at 8.3 cm^{-1} and we question their EPR analysis, which does not account properly either for the finite absorption at zero field or for the signal intensity. Our fits to the temperature-dependent EPR data and, independently, the magnetization data require that the next higher doublet in energy above the ground doublet be at approximately 20 cm^{-1}; more than a factor of 2 higher than the value (8.3 cm^{-1}) from the MCD study.[7] This discrepancy accounts for the previously reported lower D_i value of 3 cm^{-1} in comparison to our finding of 12 cm^{-1}.

To account for the finite absorption intensity at zero field in the integer-spin EPR signal, the X- and Q-band spectra require that a fraction of the molecules have Δ greater than 0.3 and 1.2 cm^{-1}, respectively. The values $|J| > 2$ cm^{-1} and $D_i = -3$ cm^{-1}, taken from the previous work,[7] give Δ values no larger than 0.08 cm^{-1}, in which case the entire signal would be seen at fields greater than zero even at X-band. However, the present values for these parameters do give the correct magnitude of Δ as demonstrated by the simulations of Figures 4 and 5. In particular, the present parameters properly account for the finite absorption at zero field at both X- and Q-band.

The previous interpretation[7] of the integer-spin EPR signal of deoxyhemerythrin azide underestimates the signal intensity by many orders of magnitude.[8,11] The present treatment yields a quantitation for the integer-spin EPR signal consistent with both optical and saturation magnetization measurements of the same sample.

The EPR signal of a ferromagnetically coupled diiron center such as deoxyhemerythrin azide is much sharper and 1–2 orders of magnitude more intense than signals from monoferrous complexes. These differences are attributable to two factors. First, the transition probability, w, for diiron centers is approximately four times larger than that from the $|2^\pm\rangle$ doublet of a monoferrous $S = 2$ quintet due to the increased magnetic moment from the ferromagnetic coupling. Second, identical heterogeneities in the zero-field parameters for the mononuclear center and the dinuclear center lead to a much sharper distribution in Δ for the dinuclear center. These heterogeneities are presumably due to random
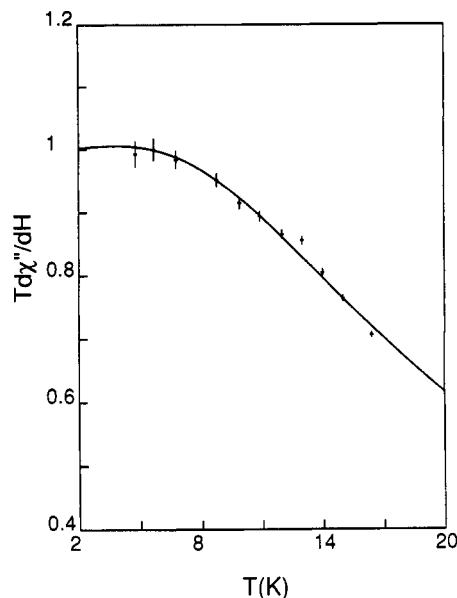
Figure 6. Temperature dependence of the deoxyhemerythrin azide EPR signal of Figure 4a. Signal intensity is determined as the depth of the valley at $H \approx 40$ mT. The theoretical line was calculated by diagonalization of eq 1 with the parameters given in Figure 4 with $\sigma_E = 0$. The error bars, in both dimensions, are dominated by the uncertainty in temperature.

variations in the iron–ligand distances. The resulting spread of the orbital energy levels is evident, through spin–orbit coupling, in the zero-field parameters. The EPR spectra are predominantly sensitive to a spread in the rhombic parameter E_i. If we assume that the mono- and diiron sites have an equal spread in the values of E_i, then the spread in Δ in the weak coupling limit relative to the spread in Δ_1 of a $S = 2$, $|2^{\pm}\rangle$ doublet is[31]

$$\sigma_\Delta = (3/4)\alpha^2(D_1/J)\sigma_{\Delta 1} \qquad (6)$$

For deoxyhemerythrin azide, eq 6 yields the result $\sigma_\Delta = (1/5)\sigma_{\Delta 1}$. The combination of the increased transition probability and sharper Δ distribution increases the intensity of the dinuclear center by a factor of 20 relative to that of ferrous mononuclear centers.[8]

The EPR spectra of integer-spin complexes are generally sensitive to one principal axis g value. For deoxyhemerythrin azide this value measured by EPR is $g_{zzi} = 2.20$ (5), which is significantly different from the spin-only value of 2.00. For d^6 ferrous, one electron above a half-filled shell, a low-lying excited orbital state will tend to unquench $\langle L \rangle$ ($\langle L \rangle \neq 0$) and raise the g value.[32] In such a situation the validity of the spin Hamiltonian (eq 1) can be questioned.[34] A test of eq 1 can be made with a relation derived from the second-order perturbation of the spin–orbit interaction[35]

$$g_{zzi} \geq 2 + (2\kappa/\lambda)(|D_i| + |E_i|) \qquad (7)$$

Using $|\lambda|/\kappa = 125$ cm^{-1}, $|D_i| = 12$ cm^{-1}, and $E_i/D_i = 0.3$, eq 7 yields $g_{zzi} \geq 2.2$. The agreement of this theoretical g value with the observed value suggests the spin Hamiltonian is valid. However, it should be stressed that these findings assume equal **g** tensors with parallel axes. The individual site g values could be considerably higher and still give an average g_{zzi} of 2.20 if one tensor is tilted relative to the other. Of course, such a tilt would also change the D_i values and may or may not result in a physical

(31) For strong coupling the relation is $\sigma_\Delta = 0.6\alpha^2\sigma_{\Delta 1}$.

(32) In contrast, the g value for the diferrous state of methane monooxygenase is 2.00[11] (the quadrupole splitting measured by Mössbauer spectroscopy is nearly temperature independent over the range 4.2–150 K[33]). The difference in g values indicates that the next higher orbital state must be at a significantly greater energy for diferrous methane monooxygenase than is the case for deoxyhemerythrin azide.

(33) Fox, B. G.; Surerus, K. K.; Münck, E.; Lipscomb, J. D. *J. Biol. Chem.* **1988**, *263*, 10553–10556.

(34) Whittaker, J. W.; Solomon, E. I. *J. Am. Chem. Soc.* **1988**, *110*, 5329–5339.

(35) Zimmermann, R.; Spiering, H.; Ritter, G. *Chem. Phys.* **1974**, *4*, 133–141.

Figure 7. Lowest quartet (see Figure 2) of energy levels versus the Euler angle β between the z axes of the zero-field splitting tensors, D_i. The lines were generated by diagonalization of eq 1 for the parameters given in Figure 4 and $H = 0$.

situation properly described by the spin-only Hamiltonian of eq 1.

The assumption that the D_i tensors of the irons are equal and parallel cannot be tested with the data presented here. Presumably, azide binds to only one of the irons, which would likely result in D_i tensors of different magnitude. While the analysis is in part sensitive to unequal, rotated D_i tensors, more data are required to make an unambiguous determination of this multidimensional parameter set. We disagree with a previous statement that allowing E_i/D_i to range beyond the conventional limits of $0 < E_i/D_i < {}^1/_3$ effectively removes the constraint of parallel axes.[7] Removing this constraint on E_i/D_i only provides 90° reorientations of the tensors leaving the axes parallel. Nor are the effects of varying the Euler angles small,[7] as can be seen from Figure 7 where the energies of the lowest four spin levels are plotted versus the Euler angle β (rotation about the y axis) between the z axes of the two iron sites. Both the splitting of the EPR-active pair and the splitting of the EPR-silent pair are strong functions of β. The analyses of both the magnetization and EPR data are compatible with the range $0 \leq \beta \leq 20°$, but this ignores the effects of the other two Euler angles.

Conclusions

Deoxyhemerythrin azide is ferromagnetically coupled as first reported by Reem and Solomon.[7] Multifield saturation magnetization data of deoxyhemerythrin azide have been used to determine the exchange coupling, average zero-field splitting, and average g value of this diferrous complex—the first time this entire set of parameters has been measured for a diferrous center. The integer-spin EPR signals at X-band, both parallel and perpendicular H_1 modes, and Q-band have been quantitatively simulated by using spin Hamiltonian parameters compatible with those measured by saturation magnetization. This is now the third case in which accurate quantitation of integer-spin EPR signals has been tested against quantitation of the same sample by other measurements.[8,16] This new quantitative capability of integer-spin EPR has been valuable in the study of methane monooxygenase[11] and may prove valuable in understanding other metalloproteins such as oxidized cytochrome c oxidase[8,14,15] and diferrous ribonucleotide reductase,[10] which are known to exhibit similar signals.